

Open Research Online

The Open University's repository of research publications
and other research outputs

Polarized P-glycoprotein expression by the immortalised human brain endothelial cell line, hCMEC/D3, restricts apical-to-basolateral permeability to rhodamine 123

Journal Item

How to cite:

Tai, Leon M.; Reddy, P. Sreekanth; Lopez-Ramirez, M. Alejandro; Davies, Heather A.; Male, A. David K.; Loughlin, A. Jane and Romero, Ignacio A. (2009). Polarized P-glycoprotein expression by the immortalised human brain endothelial cell line, hCMEC/D3, restricts apical-to-basolateral permeability to rhodamine 123. *Brain Research*, 1292 pp. 14–24.

For guidance on citations see [FAQs](#).

© 2009 Elsevier

Version: Accepted Manuscript

Link(s) to article on publisher's website:
<http://dx.doi.org/doi:10.1016/j.brainres.2009.07.039>

Copyright and Moral Rights for the articles on this site are retained by the individual authors and/or other copyright owners. For more information on Open Research Online's data [policy](#) on reuse of materials please consult the policies page.

oro.open.ac.uk

Accepted Manuscript

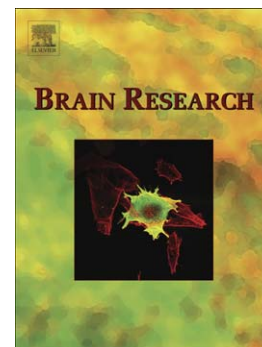
Polarized P-glycoprotein expression by the immortalised human brain endothelial cell line, hCMEC/D3, restricts apical-to-basolateral permeability to rhodamine 123

Leon M. Tai, P. Sreekanth Reddy, M. Alejandro Lopez-Ramirez, Heather A. Davies, A. David K. Male, A. Jane Loughlin, Ignacio A. Romero

PII: S0006-8993(09)01473-5
DOI: doi:[10.1016/j.brainres.2009.07.039](https://doi.org/10.1016/j.brainres.2009.07.039)
Reference: BRES 39440

To appear in: *Brain Research*

Received date: 4 March 2009
Revised date: 15 July 2009
Accepted date: 16 July 2009



Please cite this article as: Leon M. Tai, P. Sreekanth Reddy, M. Alejandro Lopez-Ramirez, Heather A. Davies, A. David K. Male, A. Jane Loughlin, Ignacio A. Romero, Polarized P-glycoprotein expression by the immortalised human brain endothelial cell line, hCMEC/D3, restricts apical-to-basolateral permeability to rhodamine 123, *Brain Research* (2009), doi:[10.1016/j.brainres.2009.07.039](https://doi.org/10.1016/j.brainres.2009.07.039)

This is a PDF file of an unedited manuscript that has been accepted for publication. As a service to our customers we are providing this early version of the manuscript. The manuscript will undergo copyediting, typesetting, and review of the resulting proof before it is published in its final form. Please note that during the production process errors may be discovered which could affect the content, and all legal disclaimers that apply to the journal pertain.

Polarized P-glycoprotein expression by the immortalised human brain endothelial cell line, hCMEC/D3, restricts apical-to-basolateral permeability to rhodamine 123

Leon M. Tai, P. Sreekanth Reddy, M. Alejandro Lopez-Ramirez, Heather A. Davies, A. David K. Male, A. Jane Loughlin, Ignacio A. Romero*

Department of Life Sciences, The Open University, Walton Hall, Milton Keynes, MK7 6AA, UK.

*Corresponding author: i.romero@open.ac.uk; Tel +44 1908 659467. Fax +44 1908 654167

Abbreviations used: ABC transporter, ATP- binding cassette transporters; BCRP, breast cancer resistance protein; BEC, brain endothelial cell; BBB, Blood-brain barrier; BSA bovine serum albumin; FITC, fluoresceine-isothiocyanate; FTC, fumitremorgin c; MTT, methylthiazolyldiphenyl-tetrazolium bromide; NGS, normal goat serum; PAF, *p*-formaldehyde; PB, phosphate buffer; P-gp, P-glycoprotein; PMSF, phenylmethylsulphonyl fluoride; rh123, rhodamine 123; EM, electron microscopy.

Abstract

P-glycoprotein (P-gp) expression at the blood-brain barrier prevents unwanted blood-borne toxins and signalling molecules from entering the brain. Primary and immortalised human brain endothelial cells (BECs) represent two suitable options for studying P-gp function *in vitro*. The limited supply of primary human BECs and their instability over passage number makes this choice unattractive for medium/high throughput studies. The aim of this study was to further characterise the expression of P-gp by an immortalised human BEC line, hCMEC/D3, in order to evaluate their use as an *in vitro* human blood-brain barrier model. P-gp expression was stable over a high passage number (up to passage 38) and was polarised on the apical plasma membrane, consistent with human BECs *in vivo*. In addition, hCMEC/D3 cell P-gp expression was comparable, albeit slightly lower to that observed in primary isolated human BECs although P-gp function was similar in both cell lines. The P-gp inhibitors tariquidar and vinblastine prevented the efflux of rhodamine 123 (rh123) from hCMEC/D3 cells, indicative of functional P-gp expression. hCMEC/D3 cells also displayed polarised P-gp transport, since both tariquidar and vinblastine selectively increased the apical-to-basolateral permeability of hCMEC/D3 cells to rh123. The results presented here demonstrate that hCMEC/D3 cells are a suitable model to investigate substrate specificity of P-gp in BECs of human origin.

Key words: P-glycoprotein, brain endothelial cells, blood brain barrier.

1. Introduction

ATP binding cassette (ABC) transporters at the blood-brain barrier (BBB) prevent the entry of unwanted endogenous signalling molecules and toxic xenobiotics from the blood into the brain [reviewed in (Loscher and Potschka, 2005)]. To date, at least 48 ABC transporter genes have been identified and are classified into seven subfamilies, denoted ABCA to ABCG (Dean et al., 2001; Higgins, 1992). ABCB1/MDR1 [(P-glycoprotein (P-gp))] is the most extensively studied ABC transporter at the BBB, both *in vitro* and *in vivo*, and prevents a broad range of substances from entering brain tissue, including many therapeutic drugs in use today such as anti-epileptics, anti-cancer drugs and HIV protease inhibitors [reviewed in (Loscher & Potschka 2005, Schinkel 1999, Zhou 2008)].

Structurally, P-gp is arranged into two halves connected by a 75 amino acid linker region, with each half consisting of a transmembrane domain (made of 6 transmembrane segments), an intracellular nucleotide-binding domain and both the N and carboxyl termini, which are located intracellularly (Linton, 2007; Schinkel, 1999; Schinkel and Jonker, 2003). Conflicting evidence exists as to the expression of P-gp by brain endothelial cells (BECs). P-gp expression has been described on the luminal membrane of rat brain capillaries (Beaulieu *et al.* 1997, Miller *et al.* 2000), isolated mouse brain endothelial cells (Tatsuta et al., 1992), and human brain microvessels (Seetharaman *et al.* 1998, Virgintino *et al.* 2002). In contrast, enhanced abluminal expression of P-gp has been observed in rat BECs using transmission electron microscopy (EM) techniques (Bendayan et al., 2006). Nevertheless, it is widely accepted that P-gp expression is primarily located on the luminal membrane of BECs.

Whilst multiple studies have been carried out to identify the characteristics of P-gp substrates, the most common feature is their hydrophobic nature, which allows

them to diffuse across the lipid bilayer relatively easily (Cabrera et al., 2006; Cianchetta et al., 2005; Crivori et al., 2006; Penzotti et al., 2002; Wang et al., 2003). Indeed, P-gp has been hypothesised to act as a flippase transporter (Schinkel, 1999). *In vivo* data supports the notion of a barrier function for P-gp at the BBB. Mice, lacking either *mdr1a* or combined *mdr1a/b* genes (equivalent to human ABCB1), display enhanced brain accumulation of many P-gp substrates including verapamil, indinavir, vinblastine and morphine, when compared to wild type control mice [reviewed in (Loscher & Potschka 2005, Miller *et al.* 2008, Schinkel 1999)]. In addition, P-gp inhibition in rats results in increased brain concentrations of colchicine and vinblastine (Drion et al., 1996).

In vivo studies represent an important data source for evaluation of ABC transporter function at the BBB, but they are highly costly and extrapolation from animal models to humans may be problematic due to species differences. For routine investigations into P-gp function by human BECs *in vitro*, there are currently two choices, primary and immortalised human BECs. Human primary cell cultures are not readily available and, in our experience, do not remain stable over ~ 5 passages, and are therefore not suited for routine medium/high throughput studies. hCMEC/D3 cells represent the most extensively characterized immortalised human BEC line to date, and retain a BEC typical phenotype (Weksler *et al.* 2005). hCMEC/D3 cells express tight junctional proteins and are restrictive to molecules larger than 4 kDa in molecular weight, in agreement with *in vivo* studies (Weksler *et al.* 2005). Previously, P-gp expression by hCMEC/D3 cells has been demonstrated using western blotting and mRNA analysis (Weksler *et al.* 2005). In the same study, an increase in the net influx of rhodamine 123 (rh123) was reported following inhibition of P-gp with PSC-

833, demonstrating that the transporter was indeed functional, as confirmed in a recent study (Poller et al., 2008).

The aim of this study was to further examine P-gp expression and function in hCMEC/D3 cells to determine their suitability as an *in vitro* human BBB model for identifying potential P-gp substrates. We first investigated P-gp expression by hCMEC/D3 cells, including its subcellular localisation and polarisation, and compared it to that of primary human BECs. P-gp functionality in hCMEC/D3 cells and primary human BECs was then investigated using rhodamine 123 (rh123) efflux, with the 3rd generation P-gp inhibitor tariquidar, or the P-gp competitive substrate vinblastine. Finally, using P-gp inhibitors, we investigated the permeability of hCMEC/D3 cells to rh123 in order to confirm polarised P-gp function.

2. Results

2.1 P-gp expression by hCMEC/D3 cells is stable and comparable to that of primary human brain endothelial cells

The levels of P-gp expression were compared between hCMEC/D3 cells at early passages (between 23 and 28) and primary human BECs (between 2 and 3) to determine the suitability of the cell line as an *in vitro* human BBB model (Fig. 1). Both primary human BECs and hCMEC/D3 cells expressed P-gp as demonstrated by a higher median fluorescence staining intensity compared to their negative controls (Fig. 1a). The levels of P-gp expression by primary human BECs were 30 % higher than those expressed by hCMEC/D3 cells, although this difference was not statistically significantly different [Fig. 1c, ($p = 0.065$)]. These results indicate that the level of expression of P-gp by hCMEC/D3 cells is close to that of primary human BECs.

The expression of P-gp by hCMEC/D3 cells over increasing passage (p) number was assessed in order to investigate stability of phenotype by this cell line (Figs. 1b and c). Using western blotting techniques, P-gp expression was detected as a diffuse band of ~ 160 kDa, reflecting different glycosylation patterns of the ABCB1 product (Ichikawa et al., 1991). P-gp expression was stable between p23 and p38, but appeared to decline at higher passages. In contrast, actin levels were maintained with the exception of the highest passage investigated (p44), whereas for P-gp expression, they declined. When normalised to actin, P-gp was stable up to p38 and decreased by ~ 35 %, between p38 and p41 (Fig. 1c).

2.2 Distribution of P-gp expression by hCMEC/D3 cells

We next investigated the sub-cellular localisation of P-gp expression by hCMEC/D3 cells. Using fluorescence microscopy, P-gp was not detected in the nucleus but appeared to be distributed throughout the cytoplasm and plasma membrane (Fig. 2). A cellular fractionation assay was then employed to investigate the relative sub-cellular distribution of P-gp. hCMEC/D3 cells were separated into cytosolic, membrane/organelle, nuclear and cytoskeletal fractions using differential detergent fractionation (Fig. 3a & b). Sp3, a transcription factor, was detected almost entirely in the nuclear fraction, whereas actin was expressed highest in the cytoskeletal fraction followed by nuclear and membrane fractions. P-gp was predominantly, although not exclusively, expressed in the membrane/organelle fraction. These results indicate that in hCMEC/D3 cells, P-gp is located on cellular membranes, which includes both the plasma membrane and membranes of intracellular organelles, in hCMEC/D3 cells.

2.3 P-gp expression is polarised to the apical membrane of hCMEC/D3 cells

P-gp expression was then investigated by transmission EM combined with immunogold staining (Fig. 4a, b & c), to determine its subcellular localisation. Immunolabelling was detected both in the cytoplasm and on the plasma membrane (with a distribution pattern of 43 %, and 57 %, respectively). However, the number of gold particles associated with the apical plasma membrane was nearly 3 times greater than that on the basolateral membrane (Fig. 4d, 66 images analysed over a 500 μ m section of membrane). Therefore, whilst P-gp molecules appear distributed on both membranes and in the cytoplasm, the majority of plasma membrane P-gp was on the apical membrane, which is consistent with the blood side *in vivo*. The localisation of P-gp to the apical plasma membrane of hCMEC/D3 cells suggests that this transporter may act to prevent the movement of P-gp substrates from the apical to the basolateral compartments in *in vitro* permeability studies.

2.4 P-gp mediates rhodamine 123 efflux by hCMEC/D3 cells

Using non-cytotoxic concentrations of the P-gp inhibitors tariquidar or vinblastine, or the Breast Cancer Resistance Protein (BCRP) inhibitor fumitremorgin c (FTC) (data not shown), rh123 efflux from preloaded hCMEC/D3 cells was investigated as a means to determine P-gp functionality in this cell line. rh123 efflux is potentially a more sensitive measure of P-gp activity than net rh123 influx, since it is exclusively dependent on the efflux activity of P-gp rather than a measure of the relative contribution of efflux versus influx mechanisms. Compared to cells preloaded with rh123 and incubated at 4 °C, cellular levels of rh123 decreased sharply within 1 h and continued to decline thereafter. The $t_{1/2}$ for rh123 efflux was estimated to be 13.3 min [$n = 3$ (Fig. 5a)]. The competitive P-gp inhibitor vinblastine (22 μ M) decreased

the rate of efflux of rh123 from hCMEC/D3 cells, [$t_{1/2} = 112.2$ min ($n = 3$)]. Both vinblastine and the allosteric P-gp inhibitor tariquidar (300 nM), but not the BCRP inhibitor FTC (22 μ M), decreased rh123 efflux from hCMEC/D3 cells pre-loaded with 22 μ M rh123 at 4°C for 60 min, and incubated at 37°C for 60 min (Fig. 5b). In addition, P-gp function in hCMEC/D3 cells was comparable to that obtained using primary hBECs over a 15 min efflux assay (Fig. 5c). These results demonstrate that rh123 efflux from hCMEC/D3 cells is largely mediated by P-gp.

Tariquidar has been demonstrated to have a long-lasting, possible irreversible, inhibitory effect on P-gp (Mistry et al., 2001), whilst vinblastine acts as a competitive inhibitor. To investigate the mechanism of P-gp inhibition by tariquidar and vinblastine, hCMEC/D3 cells were pre-loaded at 4°C with 22 μ M rh123 in the presence of either tariquidar (300 nM) or vinblastine (22 μ M), followed by incubation at 37°C for 60 min with either vehicle or inhibitors. After preloading hCMEC/D3 cells with rh123 in the presence of tariquidar, rh123 efflux was inhibited in the subsequent incubation at 37°C, with or without the continued presence of this inhibitor (cellular rh123 levels were 55.7 % \pm 4.3 and 53.7 % \pm 12.2 of cells incubated at 4°C with and without the continued presence of tariquidar, respectively, compared to 7.02 % \pm 1.82 for an ethanol control. $n = 3$, $P < 0.01$). In contrast, after loading hCMEC/D3 cells with rh123 in the presence of vinblastine, the continued presence of vinblastine during the incubation stage at 37°C was required to maintain efflux inhibition of rh123 (cellular rh123 levels compared to cells incubated at 4°C were; 50.7 % \pm 5.3 with vinblastine present during the incubation phase, 5.8 % \pm 1.4 with vinblastine absent during incubation phase and 6.2 % \pm 0.56 for DMSO control). These results confirm previous studies that tariquidar is a long lasting P-gp inhibitor which, unlike

vinblastine, can exert its effect after removal from the culture medium (Mistry et al., 2001).

2.5 P-gp restricts the apical-to-basolateral permeability of hCMEC/D3 cells to rh123

Since; 1) P-gp appeared polarised on the apical membrane of hCMEC/D3 cells, and 2) rh123 was a suitable substrate to measure P-gp function using an efflux assay, we next investigated the permeability of hCMEC/D3 cells in a two-dimensional assay, to rh123, as a guide to polarised functionality (Fig. 6). The P-gp inhibitors vinblastine and tariquidar did not significantly affect the basolateral-to-apical permeability of hCMEC/D3 cells to rh123 ($n = 3$ $P > 0.05$). However, tariquidar and vinblastine both increased hCMEC/D3 cell apical-to-basolateral permeability to rh123 by 67% and 55 % respectively, compared to control levels ($n = 3$ $P < 0.05$). These results imply that P-gp, located on the apical membrane, restricts the transport of rh123 in the apical-to-basolateral direction.

3. Discussion

Human BECs express P-gp, which acts as a barrier for many therapeutic drugs and endogenous molecules, preventing their entry into the brain [reviewed in (Loscher & Potschka 2005, Schinkel 1999)]. The study of P-gp *in vitro* using human BECs is valuable for identifying potential substrates and inhibitors. The data presented here show, that the immortalised human BEC cell line, hCMEC/D3, expresses P-gp when assessed by flow cytometry, western blotting, immunocytochemistry and immunoelectron microscopy. These data are in agreement with numerous studies that have demonstrated BEC P-gp expression at both the protein and mRNA level using *in vitro*

cultures of both primary and immortalised cells of rat, mouse and human origin (Beaulieu et al., 1997; Begley et al., 1996; Miller et al., 2000; Perriere et al., 2007; Seetharaman et al., 1998; Tatsuta et al., 1992; Virgintino et al., 2002). In terms of P-gp expression, the BEC phenotype appears to be preserved in hCMEC/D3 cells over a wide range of passages, and P-gp expression was comparable to cultured primary BECs, albeit slightly reduced. It is possible, however, that the cultured primary BECs used here have lower P-gp expression compared to isolated capillaries, which as demonstrated in rat and humans, more closely mimic the *in vivo* situation (Barrand et al., 1995; Regina et al., 1998; Regina et al., 1999; Seetharaman et al., 1998). Our observations are in agreement with those of Regina and co-workers, who reported lower expression of P-gp by an immortalised rat BEC cell line, RBE4, compared to primary rat BECs (Regina et al., 1998; Regina et al., 1999). None-the-less, the small difference in P-gp expression between for primary BECs and hCMEC/D3 cells did not result in measurable differences in P-gp function. The limited availability and stability of primary human cells, and the species differences between rat and human, makes hCMEC/D3 cells an attractive option for the study of P-gp function and identification of potential substrates over a large passage range.

In this study, differential detergent fractionation of hCMEC/D3 cells showed that P-gp expression was localised to the membrane/organelle fraction. Using transmission EM and immunogold staining, P-gp was found to be localised mainly in or at the apical membrane, although labelling in the cytoplasm and in the basolateral membrane was also observed. Using EM techniques, we found ~40 % P-gp expression in the cytoplasm of hCMEC/D3 cells, an observation that may reflect an intracellular P-gp pool capable of plasma membrane translocation under certain conditions. Indeed, some immunolabelling appeared localized to intracellular vesicles

(Fig. 4a). However, it is also possible that the intracellular P-gp staining represents internalised P-gp targeted for degradation, or newly synthesised P-gp in transit towards the plasma membrane.

These results are in partial agreement with studies from rat brain tissue, (Bendayan et al. 2006) where abluminal, luminal and intracellular membrane associated (cytoplasmic vesicles, Golgi complex, and rough endoplasmic reticulum) staining of P-gp was detected. However, in contrast to our study, Bendayan reports enhanced abluminal polarisation of P-gp in rats and much greater numbers of gold particles per μm of membrane (1.17 ± 0.04 abluminal, 0.85 ± 0.03 luminal, compared to 0.038 ± 0.009 basolateral and 0.11 ± 0.17 apical, respectively, in this study). The greater number of gold-particles found in the study by Bendayan *et al.* compared to this study, might reflect species differences between rats and humans. The antibody C219 recognises P-gp epitopes that differ slightly between rats and humans, with potentially a higher affinity for the rodent N-terminal domain (Georges et al., 1990). However, in agreement with the results reported in this study, and in contrast to the work of Bendayan *et al.*, numerous lines of evidence point to the polarisation of P-gp on the luminal membrane of BECs in rats and humans. Luminal P-gp expression has been observed in isolated human brain capillaries (Seetharaman et al., 1998), human tissue (Virgintino et al., 2002), and isolated capillaries from rats (Beaulieu et al., 1997; Miller et al., 2000). The differing results of Bendayan et al to those of others in the field, including the present study, might relate to the method of fixation. Manoonkitiwongsa *et al* (Manoonkitiwongsa et al., 2000) have demonstrated that for Na^+ , K^+ ATPase staining, with an increasing concentration of fixative (that has deleterious effects on antibody recognition), the staining decreased to a greater degree on the luminal than abluminal side. Therefore, it is possible that, when brain tissue

pieces were immersed in fixative (Bendayan *et al*), there would have been greater exposure to fixative on the luminal than abluminal sides due to the differences in tissue densities and hence diffusion of fluid, whereas with hCMEC/D3 cells cultured on inserts there would have been equal exposure.

The results presented here also confirm functional P-gp expression by hCMEC/D3 cells. The $t_{1/2}$ obtained here for rh123 efflux (~13 min) is in agreement with another study that found a $t_{1/2}$ of similar magnitude in rat primary BECs (~ 10 min) (Ji *et al.*, 2005). However, in contrast to the relatively modest increase in the efflux $t_{1/2}$ caused by another competitive inhibitor, verapamil, in that study ($t_{1/2}$ ~ 20 min), in the present study vinblastine caused a much more potent inhibition ($t_{1/2}$ ~ 110 min). Several factors may contribute to the differences in P-gp inhibition between this study and the one by Ji *et al.*: 1) differences in P-gp expression levels between rat and hCMEC/D3 cells; 2) levels of ATP in the culture media; 3) differences in the method employed for rh123 efflux. With regards to the latter, Ji *et al* preloaded rat BECs at 37°C rather than 4°C as used in this current study and the data were expressed as a percentage of time zero. However, rh123 cellular levels at 37°C would be influenced not only by passive diffusion, but also by active efflux transport making interpretation of results difficult. Since vinblastine and tariquidar both inhibited efflux of rh123, there is strong evidence that rh123 efflux from hCMEC/D3 cells is largely mediated by P-gp.

In agreement with other studies, FTC, a BCRP inhibitor, did not inhibit rh123 efflux (Weksler *et al.*, 2005; Zhang *et al.*, 2003). BCRP has been demonstrated to use rh123 as a substrate only when there is a mutation at position 482, characteristic of tumour cells (Alqawi *et al.*, 2004; Sarkadi *et al.*, 2004). Therefore, it is likely that hCMEC/D3 cells express wild type, non-mutated BCRP, since BCRP activity has

previously been demonstrated in hCMEC/D3 cells (Weksler et al. 2005). In addition, the inhibition of P-gp function by tariquidar was longer-lasting than that of vinblastine. This observation is in agreement with Mistry *et al* (Mistry et al., 2001), who reported a long-lasting inhibition of rh123 and ³H-daunorubicin efflux by tariquidar in a human ovarian carcinoma cell line, even if the inhibitor was only present in the pre-loading stage. This evidence suggests that tariquidar might be a more suitable inhibitor than vinblastine for the study of the role of P-gp in the penetration of the CNS by drugs.

Using a more relevant model of BBB transport, whereby hCMEC/D3 cells are grown on filters, we have demonstrated that P-gp restricts the apical-to-basolateral permeability of hCMEC cells to rh123. These data support our observation that P-gp appears localised to the apical plasma membrane in hCMEC/D3 cells as assessed by EM techniques and immunogold staining. In agreement, we have also recently reported that P-gp restricts the apical-to-basolateral, but not basolateral-to-apical, permeability of hCMEC/D3 cells to A β 1-40 (Tai et al., 2009). The restriction in apical-to-basolateral permeability that P-gp affords to BECs *in vitro* is consistent with the observation that, *in vivo*, mdr1a or mdr1a/b knock-out mice display enhanced CNS accumulation of many P-gp substrates, including cyclosporin A, vinblastine, digoxin, morphine and digoxin, colchicine and morphine [reviewed in (Loscher & Potschka 2005, Schinkel 1999)]. The polarised nature of P-gp function has been demonstrated *in vitro* on isolated BECs grown on filter inserts, which show directional transport of cyclosporin A and vincristine in mouse BECs (Shirai et al., 1994; Tatsuta et al., 1992).

In summary, functional P-gp expression has been demonstrated in the human immortalised cell line, hCMEC/D3. Importantly, hCMEC/D3 cells express P-gp

polarised on the apical membrane, which restricts endothelial permeability to rh123 in the apical-to-basolateral direction.

4. Experimental procedures

4.1. Materials

Tariquidar was a kind gift from Xenova (Slough, Berkshire, UK), Fumetrimorgan C (FTC) was from Axxora (Nottingham, Nottinghamshire, UK). Tissue culture plastic was from Greiner (Gloucestershire, UK). All other reagents were from Sigma-Aldrich (Gillingham, Dorset, UK) unless stated.

4.2. Isolation of human brain endothelial cells

In procedures approved by both Kings College London and The Open University local ethical committee guidelines (Protocol 99-002), human brain tissue was obtained with written consent from patients undergoing cerebral cortical lobectomies, conducted at Kings College Hospital to relieve medically intractable seizures. The isolation of human BECs was carried out as described by Weksler *et al* (Weksler et al. 2005). Briefly, brain tissue was freed of meninges, finely chopped and dispersed by enzymatic digestion in Ca^{++} and Mg^{++} -free Hanks buffered saline solution (HBSS w/o $\text{Ca}^{++}/\text{Mg}^{++}$), containing 1 mg/ml collagenase/dispase (Roche, Paisley, Renfrewshire UK), 20 U/ml DNase I and 0.15 $\mu\text{g}/\text{ml}$ tosyl-lysyl-chloromethylketone for 1 h at 37°C. Microvessel fragments were separated by density-dependent centrifugation on 25% bovine serum albumin (BSA) and subjected to a second digestion in collagenase/dispase solution at 37°C for 2 h. The microvessel fragment suspension was then centrifuged over a preformed 50 % Percoll gradient, washed and plated onto collagen-coated tissue culture plastic. To eliminate non-

endothelial cells, puromycin (0.5 µg/ml) was added to the culture medium for the first three days following isolation.

4.3. Cell culture

hCMEC/D3 and primary human BECs were cultured in EGM- 2 medium (Lonza, Slough, Wokingham, UK) supplemented with VEGF, IGF, bFGF, hydrocortisone, ascorbate, gentamycin and 2.5 % fetal bovine serum (FBS) as indicated by the manufacturer. Cells were grown on collagen-coated (5 mg/ml, 1h RT) tissue culture plastic in a humidified atmosphere at 37°C in 5 % CO₂. For all experiments, BECs were grown to confluence and left for 2 days prior to treatment (~ 1 x 10⁵ cells / cm²), with the EGM-2 medium changed every 2-3 days.

4.4. Western blotting

Confluent hCMEC/D3 cells were lysed in 500 µl of RIPA buffer containing 1 mM phenylmethylsulphonyl fluoride (PMSF) and 10 ng/ml of aprotinin, leupeptin and pepstatin A. Protein levels were measured by the Biorad DC protein assay (Hemel Hempstead, Hertfordshire, UK). Samples were denatured in 1 x Laemmli's buffer and 20 µg of protein were loaded on SDS-PAGE gels appropriate for the molecular weight of each protein under investigation. Proteins were resolved and transferred to a nitrocellulose membrane. After incubation with primaries antibodies overnight at 4°C (Table 1), membranes were incubated with a species-specific secondary antibody conjugated to horseradish peroxidase for 1 h at room temperature [1 in 10,000 dilution (Pierce Biotechnology, Tattenhoe, Cheshire, UK)], and were visualised by enhanced chemiluminescence detection (ECL, Amersham, Buckinghamshire, UK). For some blots, to confirm equal loading, membranes were stripped in buffer [2 % (w/v) SDS,

0.0625 M Tris pH 6.8, 0.008 % (v/v) β -mercaptoethanol] and re-probed with mouse monoclonal anti-actin (1 μ g/ml). The signal intensities of the bands were then normalised to actin.

4.5. Differential detergent fractionation

hCMEC/D3 whole cell lysates were separated into cytosolic, membrane/organelle, nuclear and cytoskeletal fractions using differential detergent fractionation as described by Ramsby *et al* (Ramsby et al., 1994). Briefly, hCMEC/D3 cells were grown to confluence in 75 cm² flasks, washed in HBSS w/o Ca⁺⁺/Mg⁺⁺ and detached with 0.25 % v/v porcine trypsin and 0.02 % w/v EDTA. After centrifugation (500 x g, 10 min, 4°C), cells were lysed at 4°C in 250 μ l of 10 mM piperazine- 1, 4'-bis (2-ethanesulphonic acid) (PIPES) buffer pH 6.8, containing 300 mM sucrose, 100 mM NaCl, 3 mM MgCl₂, 5 mM EDTA, 1.2 mM PMSF and 0.01 % w/v digitonin. After centrifugation (500 x g, 10 min, 4°C), supernatants (cytosolic protein fraction) were collected and the pellets were re-suspended on ice for 20 min in 250 μ l of 10 mM PIPES pH 7.4 buffer containing 300 mM sucrose, 100 mM NaCl, 3 mM MgCl₂, 3 mM EDTA, 1.2 mM PMSF and 0.5 % v/v triton X-100. After centrifugation (5000 x g, 10 min, 4°C), supernatants (containing membrane/organelle fraction) were collected and the remaining pellets were re-suspended on ice for 10 min in 125 μ l of a 10 mM PIPES pH 7.4 buffer containing 10 mM NaCl, 1 mM MgCl₂, 1.2 mM PMSF, 0.5 % v/v triton X-100, 1 % v/v tween-40 and 0.5 % wt/vol sodium deoxycholate. After centrifugation (7000 x g, 10 min, 4°C), supernatants (containing nuclear proteins) were collected, whilst the pellet contained the cytoskeletal proteins. All fractions were dissolved in 1 x Laemmli's buffer. Aliquots for each subcellular

fraction equivalent to the same cell sample were loaded on SDS-PAGE gels and subjected to electrophoresis and immunoblotting as described above.

4.6. Flow cytometry

Fully confluent hCMEC/D3 and primary BECs were detached as described above and fixed in 4 % w/v *p*-formaldehyde (PAF) for 10 min. After one wash in phosphate buffer saline (PBS), cells were blocked and permeabilised for 30 min [0.1 % w/v triton X-100, 3 % w/v normal goat serum (NGS) in PBS], then incubated overnight at 4°C with an anti-P-gp antibody (see Table 1) or an isotype-matched antibody as a negative control. hCMEC/D3 cells were then washed three times in PBS and incubated with 10 µg/ml of a fluorescein inisothiocyanate (FITC) - conjugated goat anti-mouse IgG antibody (Chemicon, Chandlers Ford, Hampshire, UK). After two final washes with PBS, the cells were suspended in 500 µl PBS and analysed using a FACSCalibur flow cytometer with Cellquest software [488 nm $\lambda_{\text{excitation}}$, 530 nm $\lambda_{\text{emission}}$, (Becton Dickinson, Oxford, Oxfordshire, UK)]. For each sample the median fluorescence of 10,000 cells was determined.

4.7. Immunocytochemistry

hCMEC/D3 cells were grown to fully confluence on collagen coated glass coverslips (5 mg/ml, 1 h). Cells were then fixed in methanol at -20°C for 10 min, and washed 3 times in PBS. An anti-P-gp antibody (Table 1) or isotype matched control antibody was then added to the fixed cells overnight at 4°C. After three 10 min washes in PBS, a 1 in 100 dilution of Alexa Fluor-555 (Molecular probes, Eugene, Oregon, US) conjugated goat anti-mouse antibody was added for 1 h at RT. After 2

final washes in PBS, the slides were mounted and viewed with a fluorescence microscope (Olympus, Watford, Hertfordshire, UK).

4.8. Transmission electron microscopy combined with immunogold labelling

For the detection of P-gp at the ultrastructural level, the method of Bendayan *et al* (Bendayan *et al.*, 2006) was followed with modifications. Briefly, hCMEC/D3 cells were grown to confluence on collagen- and fibronectin- coated transwell polyester membrane inserts and left for 2 days. hCMEC/D3 cells were then fixed for 21 h (6 h RT, 15 h 4°C) in phosphate buffer (PB) containing 2 % w/v PAF, 0.01 M sodium *m*-periodate and 0.075 M lysine. Post fixation, hCMEC/D3 cells were washed twice with PB (1–5 min), cut into 2 mm strips and processed using ‘progressive lowering of temperature’ with a Leica AFS2 automatic freeze substitution system (Leica, Milton Keynes, Buckingham UK). This method involves the progressive lowering of temperature from 0° to -30°C whilst increasing the methanol content of the solution. hCMEC/D3 cells were infiltrated in the acrylic resin Lowicryl K4M (Agar Scientific, Essex, UK) and polymerised at -30°C under ultra violet (UV) light. Ultrathin 80 nm sections of the membrane insert were then cut using a Diatome diamond knife on a Leica ultra-microtome (Leica UCT, Leica, Buckinghamshire UK). The sections were mounted on formvar (Agar Scientific, Stanstead, Essex, UK) coated nickel slot grids. Non-specific binding was blocked using 1 % (w/v) ovalbumin in 0.01 M PBS for 30 min at RT. Grids were incubated with droplets of an anti-P-gp antibody (Table 1) or an isotype-matched control overnight at RT, washed (three times for 5 min in PBS), blocked (1 % w/v ovalbumin, 10 min , RT) and incubated with a goat anti-mouse IgG secondary antibody conjugated to 10 nm gold particles for 2 h at RT (British Biocell International, Cardiff, Cardiff, Wales). The

samples were then washed (three times for 5 min in PBS), fixed in 2.5 % w/v glutaraldehyde in PBS (Agar Scientific, Stanstead, Essex, UK), washed (twice for 5 min in PBS then 1 min with deionised water), allowed to air dry and counterstained with 4 % w/v aqueous uranyl acetate (Agar Scientific, Essex, UK) for 15 min. After a final three washes in distilled water the sections were examined using a JEOL JEM 1400 transmission electron microscope operating at 80 kV. The images were acquired using an AMT XR60 11 mega pixel digital camera calibrated for magnification such that each image displayed a scale marker. Images of 7.5 μm lengths of membrane were taken every 2-3 frames for a total of 500 μm membrane. For both the apical and basolateral membranes, the number of gold particles within 100 nm of the membrane were counted in each 7.5 μm length of membrane and expressed as gold particles per 1 μm of plasma membrane. The number of cytoplasmic gold particles not within 100 nm of the plasma membrane were also counted, and expressed as a percentage of total gold particles.

4.9. Rhodamine 123 efflux assay

hCMEC/D3 cells were grown to confluence and detached. 1×10^6 cells/ml hCMEC/D3 cells were preloaded by incubation with efflux buffer [RPMI-1640, (Lonza, Slough, Wokingham, UK) containing 1 % w/v BSA] containing 10 $\mu\text{g}/\text{ml}$ (22 μM) rh123 on ice for 1 h. Rh123-preloaded cells were washed twice in efflux buffer and redistributed into different tubes for each test condition (2.5×10^5 cells were used for each sample). Duplicate tubes were placed at 4°C in efflux buffer, whilst the remaining tubes were incubated at 37°C in the presence of vinblastine (22 μM dissolved in DMSO) or DMSO only in efflux buffer. At 15, 30, 60, 120, 180 and 360 min intervals, tubes containing 2.5×10^5 cells were removed and placed on ice for

the remainder of the experiment. After all samples had been collected, cells were washed twice in PBS and resuspended in 500 μ l PBS. Cell samples were then read using a FACSCalibur with Cellquest software (Becton Dickson) and the median fluorescence of 10,000 cells per sample recorded. The median fluorescence intensity of a negative control (cells not loaded with rh123) was subtracted from all the other treatments and the data expressed as a percentage of rh123 preloaded cells kept at 4°C. For some experiments, the effect of vinblastine [competitive P-gp and MRP-1 inhibitor (22 μ M)], tariquidar [specific P-gp inhibitor (300 nM dissolved in ethanol)] or FTC (competitive BCRP inhibitor (22 μ M, dissolved in DMSO)] on rh123 accumulation in hCMEC/D3 cells or primary hBECs incubated at 37°C for the indicated periods of time was tested. In these experiments, cells were preloaded with either rh123 alone or in the presence of an inhibitor.

4.10. Rh123 permeability assay

hCMEC/D3 cells were grown to confluence on transwell polyester membrane inserts [Corning Costar, High Wycombe, Buckinghamshire, UK (0.4 μ m pore, 12mm diameter)], which were first coated with collagen as before and then with fibronectin (5 μ g/ml for 1 h). The paracellular permeability to rh123 of the hCMEC/D3 monolayers was then investigated. Briefly, 2 μ M rh123 and 0.1 mM 14 C Inulin [1-3 μ Ci/mg (MP biomedical, Solon, Ohio, USA)] alone or in the presence of tariquidar (300 nM), or vinblastine (22 μ M) was added to the apical chamber, and the fluorescence and β -emission counter that crossed to the basolateral chamber was determined over 30 min, in successive 5 min periods, using a BMG plate reader (Offenberg, Germany) and β -counter (Wallac triluX, Perkin Elmer, Cambridge, Cambridgeshire, UK). The volume cleared was plotted against time, and the slopes of

the curves used to calculate the permeability coefficients (P_e , cm/min) of the endothelial cell monolayer:

$P_e = PS/s$, where PS (clearance) is the permeability surface area of the endothelial monolayer and s is the surface area of the filter (1.1 cm^2).

PS is given by: $1/PS = 1/m_e - 1/m_f$, where m_e and m_f are the slopes of the curves corresponding to endothelial cells on filters and to filters only, respectively. m_e and m_f were calculated by plotting the cleared volume against time.

The cleared volume was calculated by: $(AU_a - AU_b)/F_i$, where AU_a is the total fluorescence (arbitrary units) in the basal compartment, AU_b is the background fluorescence and F_i is the fluorescence of the initial solution (AU/ml).

To investigate the basolateral-to-apical permeability, 1.5 ml rh123 ($22 \mu\text{M}$) and $0.1 \text{ mM } ^{14}\text{C}$ Inulin was added to the basolateral chamber of a 12 well plate [\pm tariquidar (300 nM), vinblastine ($22 \mu\text{M}$) or FTC ($22 \mu\text{M}$)] and filters containing the appropriate inhibitors placed into the well. The filter was left in place for 30 min and the fluorescence and β -emission of the apical and basolateral chambers measured. The P_e values were calculated using the assumption that the curve was linear:

$$PS_{ef} = [(AU_a - AU_b)/F_i] / 30$$

In order to eliminate the influence of paracellular leakage of in the rh123 permeability experiments, a clearance quotient was calculated using the following formula;

$$\text{Rh123 CQ} = \frac{P_e \text{ Rh123}}{P_e \text{ } ^{14}\text{C inulin}}$$

$$P_e \text{ } ^{14}\text{C inulin}$$

4.11. Statistical analysis

All data are represented as means \pm SEM and the number of experiments, n , is indicated each time. Statistical significance was determined using ANOVA followed by Student's t test, comparing each treatment to the appropriate control (* $P < 0.05$). For rh1213 permeability, a paired t test was used, since the data was paired.

Fig. 1. The expression of P-gp by hCMEC/D3 and primary hBECs . (a) Fully confluent hCMEC/D3 cells (passage 23-28) and primary hBECs (passage 2-4) were fixed in 4% PAF, permeabilised using 0.1% triton X-100 and stained with antibodies for P-gp (JSB-1, mouse monoclonal IgG₁) or an isotype matched negative control (mouse IgG₁), and analysed via flow cytometry. Data represents mean \pm SEM, n = 3 with duplicate samples. ** $P < 0.01$ using Student's t test (b) Immunoblots of hCMEC/D3 cell whole cell lysates stained with antibodies for P-gp and actin between passage 23 and 44. (c) The signal intensity of the bands corresponding to P-gp and actin were determined using Image J software and P-gp expression was normalised against actin. Results from one experiment.

Fig. 2. Expression of P-gp by hCMEC/D3 cells as viewed by fluorescence microscopy. hCMEC/D3 cells (p 28) were grown to confluence on collagen coated glass coverslips. Cells were fixed, permeabilised and stained for P-gp using either the antibody C219 (b), or JSB-1 (d) or isotype matched controls (a,c), as described in the Methods. Images are from one experiment representative of three. Scale bar represents 50 μ m.

Fig. 3. Sub-cellular distribution of P-gp by hCMEC/D3 cells as assessed by differential detergent fractionation. (a) Fully confluent hCMEC/D3 cells were separated into 1) cytosol, 2) membrane/organelle, 3) nuclear and 4) cytoskeletal components using differential detergent fractionation and the expression of Sp3, actin and P-gp was assessed by western blotting. (b) Relative expression of each protein in cytosol, membrane/organelle, nuclear and cytoskeletal fractions as a percentage of total expression. Data represents mean \pm SEM, n = 3.

Fig. 4. The expression of P-gp as detected via transmission electron microscopy and immunogold labelling. hCMEC/D3 cells (p 28) were grown to confluence on transwell polyester membrane inserts and stained for P-gp as described in the Methods. a, b, and c are representative images of gold particles found intracellularly and on the basolateral and apical membranes, respectively. (d) One frame length of 7.5 μm was taken every 2-3 frames for a total of 500 μm , and the number of gold particles counted within 100 nm (shown as scale bar) of the apical or basolateral membrane was quantified. * $P < 0.05$, ** $P < 0.01$, *** $P < 0.001$ using Student's t test. Arrows indicate immunolabelling with gold particles.

Fig. 5. Time-dependent efflux of rh123 by hCMEC/D3 cells. (a) Fully confluent hCMEC/D3 cells were preloaded with rh123 (22 μM) for 1 h at 4°C and then incubated at 37°C in the presence of 22 μM vinblastine or DMSO (control) for 15, 30, 60, 120, 180 or 360 min. The cells were analysed by flow cytometry (488 nm $\lambda_{\text{excitation}}$ 520 nm $\lambda_{\text{emission}}$). The median fluorescence intensity was measured and expressed as a percentage of preloaded cells incubated at 4°C. (b and c) hCMEC/D3 or (c) primary human BECs were preloaded with rh123 (22 μM) at 4°C for 60 min followed by (b) 60 min or (c) 15 min incubation at 37 °C in the presence of tariquidar (300 nM), vinblastine (22 μM), FTC (22 μM) or an appropriate control and the median fluorescence intensity measured by flow cytometry. Data represents mean \pm SEM, n = 3 with duplicate samples for hCMEC/D3 cells (a, b and c) and n=3 from two different donors for primary hBEC (c). * $P < 0.05$, ** $P < 0.01$ using Student's t test.

Fig. 6. The permeability of hCMEC/D3 cells to rh123 in the presence or absence of tariquidar and vinblastine. hCMEC/D3 cell were grown to confluence on collagen- and fibronectin- coated filter inserts. rh123 (22 μ M) and 0.1 mM 14 C Inulin was then added to the apical or basolateral side of the filter in the presence of tariquidar (300 nM), vinblastine (22 μ M) or DMSO control. The rh123 clearance quotient was then calculated as described in the methods section. Data represents mean \pm SEM, n = 4 (a), or 3 (b) with duplicate samples. * $P < 0.05$ using a paired t-test.

- Alqawi, O., Bates, S., Georges, E., 2004. Arginine482 to threonine mutation in the breast cancer resistance protein ABCG2 inhibits rhodamine 123 transport while increasing binding. *Biochem J.* 382, 711-6.
- Barrand, M.A., Robertson, K.J., von Weikersthal, S.F., 1995. Comparisons of P-glycoprotein expression in isolated rat brain microvessels and in primary cultures of endothelial cells derived from microvasculature of rat brain, epididymal fat pad and from aorta. *FEBS Lett.* 374, 179-83.
- Beaulieu, E., Demeule, M., Ghitescu, L., Beliveau, R., 1997. P-glycoprotein is strongly expressed in the luminal membranes of the endothelium of blood vessels in the brain. *Biochem J.* 326 (Pt 2), 539-44.
- Begley, D.J., Lechardeur, D., Chen, Z.D., Rollinson, C., Bardoul, M., Roux, F., Scherman, D., Abbott, N.J., 1996. Functional expression of P-glycoprotein in an immortalised cell line of rat brain endothelial cells, RBE4. *J Neurochem.* 67, 988-95.
- Bendayan, R., Ronaldson, P.T., Gingras, D., Bendayan, M., 2006. In situ localization of P-glycoprotein (ABCB1) in human and rat brain. *J Histochem Cytochem.* 54, 1159-67.
- Cabrera, M.A., Gonzalez, I., Fernandez, C., Navarro, C., Bermejo, M., 2006. A topological substructural approach for the prediction of P-glycoprotein substrates. *J Pharm Sci.* 95, 589-606.
- Cianchetta, G., Singleton, R.W., Zhang, M., Wildgoose, M., Giesing, D., Fravolini, A., Cruciani, G., Vaz, R.J., 2005. A pharmacophore hypothesis for P-glycoprotein substrate recognition using GRIND-based 3D-QSAR. *J Med Chem.* 48, 2927-35.
- Crivori, P., Reinach, B., Pezzetta, D., Poggesi, I., 2006. Computational models for identifying potential P-glycoprotein substrates and inhibitors. *Mol Pharm.* 3, 33-44.

- Dean, M., Hamon, Y., Chimini, G., 2001. The human ATP-binding cassette (ABC) transporter superfamily. *J Lipid Res.* 42, 1007-17.
- Drion, N., Lemaire, M., Lefauconnier, J.M., Scherrmann, J.M., 1996. Role of P-glycoprotein in the blood-brain transport of colchicine and vinblastine. *J Neurochem.* 67, 1688-93.
- Georges, E., Bradley, G., Gariepy, J., Ling, V., 1990. Detection of P-glycoprotein isoforms by gene-specific monoclonal antibodies. *Proc Natl Acad Sci U S A.* 87, 152-6.
- Higgins, C.F., 1992. ABC transporters: from microorganisms to man. *Annu Rev Cell Biol.* 8, 67-113.
- Ichikawa, M., Yoshimura, A., Furukawa, T., Sumizawa, T., Nakazima, Y., Akiyama, S., 1991. Glycosylation of P-glycoprotein in a multidrug-resistant KB cell line, and in the human tissues. *Biochim Biophys Acta.* 1073, 309-15.
- Ji, B.S., He, L., Liu, G.Q., 2005. Modulation of P-glycoprotein function by amlodipine derivatives in brain microvessel endothelial cells of rats. *Acta Pharmacol Sin.* 26, 166-70.
- Linton, K.J., 2007. Structure and function of ABC transporters. *Physiology (Bethesda).* 22, 122-30.
- Loscher, W., Potschka, H., 2005. Role of drug efflux transporters in the brain for drug disposition and treatment of brain diseases. *Prog Neurobiol.* 76, 22-76.
- Manoonkitiwongsa, P.S., Schultz, R.L., Wareesangtip, W., Whitter, E.F., Nava, P.B., McMillan, P.J., 2000. Luminal localization of blood-brain barrier sodium, potassium adenosine triphosphatase is dependent on fixation. *J Histochem Cytochem.* 48, 859-65.

- Miller, D.S., Nobmann, S.N., Gutmann, H., Toeroek, M., Drewe, J., Fricker, G., 2000. Xenobiotic transport across isolated brain microvessels studied by confocal microscopy. *Mol Pharmacol.* 58, 1357-67.
- Mistry, P., Stewart, A.J., Dangerfield, W., Okiji, S., Liddle, C., Bootle, D., Plumb, J.A., Templeton, D., Charlton, P., 2001. In vitro and in vivo reversal of P-glycoprotein-mediated multidrug resistance by a novel potent modulator, XR9576. *Cancer Res.* 61, 749-58.
- Penzotti, J.E., Lamb, M.L., Evensen, E., Grootenhuys, P.D., 2002. A computational ensemble pharmacophore model for identifying substrates of P-glycoprotein. *J Med Chem.* 45, 1737-40.
- Perriere, N., Yousif, S., Cazaubon, S., Chaverot, N., Bourasset, F., Cisternino, S., Decleves, X., Hori, S., Terasaki, T., Deli, M., Scherrmann, J.M., Temsamani, J., Roux, F., Couraud, P.O., 2007. A functional in vitro model of rat blood-brain barrier for molecular analysis of efflux transporters. *Brain Res.* 1150, 1-13.
- Poller, B., Gutmann, H., Krahenbuhl, S., Weksler, B., Romero, I., Couraud, P.O., Tuffin, G., Drewe, J., Huwyler, J., 2008. The human brain endothelial cell line hCMEC/D3 as a human blood-brain barrier model for drug transport studies. *J Neurochem.* 107, 1358-68.
- Ramsby, M.L., Makowski, G.S., Khairallah, E.A., 1994. Differential detergent fractionation of isolated hepatocytes: biochemical, immunochemical and two-dimensional gel electrophoresis characterization of cytoskeletal and noncytoskeletal compartments. *Electrophoresis.* 15, 265-77.
- Regina, A., Koman, A., Piciotti, M., El Hafny, B., Center, M.S., Bergmann, R., Couraud, P.O., Roux, F., 1998. Mrp1 multidrug resistance-associated protein and P-

- glycoprotein expression in rat brain microvessel endothelial cells. *J Neurochem.* 71, 705-15.
- Regina, A., Romero, I.A., Greenwood, J., Adamson, P., Bourre, J.M., Couraud, P.O., Roux, F., 1999. Dexamethasone regulation of P-glycoprotein activity in an immortalized rat brain endothelial cell line, GPNT. *J Neurochem.* 73, 1954-63.
- Sarkadi, B., Ozvegy-Laczka, C., Nemet, K., Varadi, A., 2004. ABCG2 -- a transporter for all seasons. *FEBS Lett.* 567, 116-20.
- Schinkel, A.H., 1999. P-Glycoprotein, a gatekeeper in the blood-brain barrier. *Adv Drug Deliv Rev.* 36, 179-194.
- Schinkel, A.H., Jonker, J.W., 2003. Mammalian drug efflux transporters of the ATP binding cassette (ABC) family: an overview. *Adv Drug Deliv Rev.* 55, 3-29.
- Seetharaman, S., Barrand, M.A., Maskell, L., Scheper, R.J., 1998. Multidrug resistance-related transport proteins in isolated human brain microvessels and in cells cultured from these isolates. *J Neurochem.* 70, 1151-9.
- Shirai, A., Naito, M., Tatsuta, T., Dong, J., Hanaoka, K., Mikami, K., Oh-hara, T., Tsuruo, T., 1994. Transport of cyclosporin A across the brain capillary endothelial cell monolayer by P-glycoprotein. *Biochim Biophys Acta.* 1222, 400-4.
- Tai, L.M., Loughlin, A.J., Male, D.K., Romero, I.A., 2009. P-glycoprotein and breast cancer resistance protein restrict apical-to-basolateral permeability of human brain endothelium to amyloid-beta. *J Cereb Blood Flow Metab.*
- Tatsuta, T., Naito, M., Oh-hara, T., Sugawara, I., Tsuruo, T., 1992. Functional involvement of P-glycoprotein in blood-brain barrier. *J Biol Chem.* 267, 20383-91.
- Virgintino, D., Robertson, D., Errede, M., Benagiano, V., Girolamo, F., Maiorano, E., Roncali, L., Bertossi, M., 2002. Expression of P-glycoprotein in human cerebral cortex microvessels. *J Histochem Cytochem.* 50, 1671-6.

- Wang, R.B., Kuo, C.L., Lien, L.L., Lien, E.J., 2003. Structure-activity relationship: analyses of p-glycoprotein substrates and inhibitors. *J Clin Pharm Ther.* 28, 203-28.
- Weksler, B.B., Subileau, E.A., Perriere, N., Charneau, P., Holloway, K., Leveque, M., Tricoire-Leignel, H., Nicotra, A., Bourdoulous, S., Turowski, P., Male, D.K., Roux, F., Greenwood, J., Romero, I.A., Couraud, P.O., 2005. Blood-brain barrier-specific properties of a human adult brain endothelial cell line. *Faseb J.* 19, 1872-4.
- Zhang, W., Mojsilovic-Petrovic, J., Andrade, M.F., Zhang, H., Ball, M., Stanimirovic, D.B., 2003. The expression and functional characterization of ABCG2 in brain endothelial cells and vessels. *Faseb J.* 17, 2085-7.

Anti-	Species	WB	ICC	FC	TEM	Source
P-gp (C219)	Mouse monoclonal IgG _{2a}	500 ng/ml	5 µg/ml	-	5 µg/ml	Abcam, Cambridgeshire, UK
P-gp (JSB1)	Mouse monoclonal IgG ₁	-	5 µg/ml	5 µg/ml	-	Abcam, Cambridgeshire, UK
SP3	Mouse monoclonal IgG _{2a}	200 ng/ml	-	-	-	Santa Cruz, California, USA
β-actin	Mouse monoclonal IgG ₁	1 µg/ml	-	-	-	Sigma-Aldrich, Dorset, UK
-	Mouse monoclonal IgG ₁	-	5 µg/ml	5 µg/ml	-	Sigma-Aldrich, Dorset, UK
-	Mouse monoclonal IgG _{2a}	-	5 µg/ml	-	5 µg/ml	Sigma-Aldrich, Dorset, UK

Table 1. Antibodies and concentrations used in this study. WB, western blotting; ICC, immunocytochemistry; FC, flow cytometry; TEM, transmission electron microscopy.

